

Marquette University

e-Publications@Marquette

Biomedical Sciences Faculty Research and
Publications

Biomedical Sciences, Department of

2-2022

Craniofacial Fluctuating Asymmetry in Gorillas, Chimpanzees, and Macaques

Ashly N. Romero

D. Rex Mitchell

Siobhán B. Cooke

Claire A. Kirchhoff

Claire E. Terhune

Follow this and additional works at: https://epublications.marquette.edu/biomedsci_fac



Part of the [Neurosciences Commons](#)

Marquette University

e-Publications@Marquette

Biomedical Sciences Faculty Research and Publications/College of Health Sciences

This paper is NOT THE PUBLISHED VERSION.

Access the published version via the link in the citation below.

American Journal of Biological Anthropology, Vol. 177, No. 2 (February 2022): 286-299. [DOI](#). This article is © 2022 Wiley and permission has been granted for this version to appear in [e-Publications@Marquette](#). Wiley does not grant permission for this article to be further copied/distributed or hosted elsewhere without express permission from Wiley.

Craniofacial Fluctuating Asymmetry in Gorillas, Chimpanzees, and Macaques

Ashly N. Romero

Department of Anthropology, University of Arkansas, Fayetteville, Arkansas

D. Rex Mitchell

College of Science and Engineering, Flinders University, Adelaide, South Australia, Australia

Siobhán B. Cooke

Department of Functional Anatomy and Evolution, Johns Hopkins University School of Medicine, Baltimore, Maryland

Claire A. Kirchhoff

Department of Biomedical Sciences, Marquette University, Milwaukee, Wisconsin

Claire E. Terhune

Department of Anthropology, University of Arkansas, Fayetteville, Arkansas

Abstract

Objectives

Craniofacial fluctuating asymmetry (FA) refers to the random deviations from symmetry exhibited across the craniofacial complex and can be used as a measure of developmental instability for

organisms with bilateral symmetry. This article addresses the lack of data on craniofacial FA in nonhuman primates by analyzing FA magnitude and variation in chimpanzees, gorillas, and macaques. We offer a preliminary investigation into how FA, as a proxy for developmental instability, varies within and among nonhuman primates.

Materials and Methods

We generated 3D surface models of 121 crania from *Pan troglodytes troglodytes*, *Gorilla gorilla gorilla*, and *Macaca fascicularis fascicularis*. Using geometric morphometric techniques, the magnitude of observed FA was calculated and compared for each individual, sex, and taxon, along with the variation of FA across cranial regions and for each bilateral landmark.

Results

Gorillas and macaques exhibited higher and more similar magnitudes of FA to each other than either taxon did to chimpanzees; variation in magnitude of FA followed this same trend. No significant differences were detected between sexes using pooled data across species, but sex did influence FA magnitude within taxa in gorillas. Further, variation in FA variance across cranial regions and by landmark was not distributed in any particular pattern.

Conclusion

Possible environmentally induced causes for these patterns of FA magnitude include differences in growth rate and physiological stress experienced during life. Developmental stability may be greatest in chimpanzees in this sample. Additionally, these results point to appropriate landmarks for future FA analyses and may help suggest more urgent candidate taxa for conservation efforts.

1 INTRODUCTION

Analysis of asymmetry, or differences in the right and left sides of bilaterally symmetric structures in the vertebrate skeleton, can provide information about organismal development. The relative degree of asymmetry is informative of an organism's ability to buffer environmental and genetic perturbation during development (i.e., developmental noise), referred to as developmental stability (Clarke, **1998**). Differences in craniofacial asymmetry, as a proxy for developmental instability, among primate species remain largely unexplored, with only humans, baboons, chimpanzees, gorillas, and macaques included in single-species or two-species studies (Hallgrímsson, **1993, 1999**; Livshits et al., **1998**; Livshits & Smouse, **1993**; Reddy, **1999**; Van Dongen, **2015**; Willmore et al., **2005**). Further, variation in craniofacial asymmetry among and within species has not been explored and is important for understanding primate evolution with potentially valuable applications for primate conservation. Here, we expand the current knowledge of asymmetry in primates by comparing the relative degree of bilateral asymmetry of three primate species (*Gorilla gorilla*, *Pan troglodytes*, and *Macaca fascicularis*) and analyzing variation in asymmetry across the cranium.

1.1 Fluctuating asymmetry

Bilateral symmetry is the expected outcome for most organisms in the clade Bilateria because both the right and left side of the body experience the same environmental conditions (Graham et al., **2010**; Klingenberg, **2003a, 2003b**). However, when developmental buffering breaks down, asymmetry, particularly fluctuating asymmetry (FA), increases. FA is a measure of the degree of random deviation

from symmetry in bilateral traits (Van Valen, **1962**). An increase in FA, therefore, indicates decreased developmental stability, and animals experiencing greater perturbation during development should exhibit more FA (Klingenberg, **2003a**, **2003b**).

FA is a nonspecific phenomenon that is potentially caused by many types of disturbances. Multiple factors have been suggested to be correlated with FA, including parasitism (Folstad et al., **1996**), malnutrition (DeLeon, **2007**; Hoover & Matsumura, **2008**), habitat destruction (Hopton et al., **2009**), sex (Schlager & Rüdell, **2015**), rate of growth (Hallgrímsson, **1998**), and other environmental stressors (Coda et al., **2017**; DeLeon, **2007**). Additionally, FA seems to influence reproductive success in some species (Møller, **1997**). Overall, increased physiological stress can increase levels of FA in individuals, which makes FA a practical choice for investigating the relationship between environmental changes and stress (Coda et al., **2017**) with potential applications for primate conservation.

Regarding the rate of growth, FA is suggested to accumulate during ontogeny in mammals (Hallgrímsson, **1993**, **1999**), so slower-growing primates accrue more disruptions to symmetry when compared to species that have shorter maturational spans. Slower growth requires more bone turnover, a passive process, which allows random asymmetry to accrue over time. In the sample for this study, gorillas and chimpanzees have longer, more similar maturational spans to each other than either do to macaques (Leigh, **1996**). Therefore, gorillas and chimpanzees may exhibit higher levels of FA than macaques. However, gorillas and macaques have higher growth constants than chimpanzees (Mumby & Vinicius, **2008**), which is a reflection of their higher growth rates and suggests that gorillas and macaques may exhibit higher levels of FA than chimpanzees. Some researchers have suggested that individuals in more stable environments (i.e., those with less noise and perturbation) may have higher FA when exposed to perturbation than those in more variable environments because there is less need for developmental stability in an environment that has relatively little disruption (Emlen et al., **1993**). Over generations, populations in stable environments may exhibit reduced FA or at least no increase in FA over time because they experience fewer perturbations.

The threshold at which perturbations during development may result in increased FA is unclear. Individuals with increased developmental stability could have higher thresholds for developmental noise, meaning they are better able to buffer these perturbations and therefore develop more symmetrically than those with lower thresholds for perturbation (Emlen et al., **1993**, **2003**). Alternatively, the amount of stress an individual experiences may be the factor determining the level of FA present in an individual's cranium (e.g., DeLeon, **2007**). It is not always possible to distinguish between these determinants, so a high amount of stress, low developmental stability, or a combination of both could cause high levels of FA.

Relatively little is known about how craniofacial FA varies within and between nonhuman primate species and the degree to which these processes are influenced by genetic and environmental factors. In the few studies on primate craniofacial FA to date, FA has been shown to be present in chimpanzees and gorillas (Singh et al., **2012**; Van Dongen, **2015**), macaques (Hallgrímsson, **1993**, **1999**), baboons (Van Dongen, **2015**), bonobos and orangutans (Singh et al., **2012**), and tamarins (Hutchison & Cheverud, **1995**). Using nonmetric traits, McGrath et al. (**1984**) found that FA is at least somewhat explained by the genetic structure in the rhesus macaque population they studied, though with low levels of heritability. Furthermore, FA and FA variance increase throughout ontogeny, and an increase

in FA has been quantified in species with extended developmental timeframes (Hallgrímsson, **1993, 1995, 1999**). Hallgrímsson suggested that this is a result of noise accumulating during ontogeny but at a level below that causing a morphogenetic mechanism. He suggested that variance increases due to morphogenetic drift and possibly functional asymmetry (i.e., asymmetry caused by mechanical loading of bone). In their quantitative genetic investigation of FA using inter-landmark distances and a Procrustes landmark dataset in rhesus macaques (*Macaca mulatta*), Willmore et al. (**2005**) found that FA increased with environmental and phenotypic variance of these distances. The relationship between FA and environmental variance was more robust than that between FA and phenotypic variance, meaning that the environment in which these macaques lived largely influenced FA based on the genetic structure of the population. They suggest that these results could mean an overlap between the processes responsible for developmental stability and canalization of traits. Canalization refers to a population-specific rather than individual-specific evolutionary phenomenon where a phenotypic trait remains similar across individuals, even with environmental and genetic differences (Willmore et al., **2007**). Their results also point to a greater relationship between environmental variables (e.g., parasite load, temperature stress, and habitat changes) and FA than genetic variables. Though these studies provide information about FA within these nonhuman primate species, none of them compared levels of FA between primate species but rather examine FA as part of a larger developmental picture.

1.2 Regional variation in FA across the cranium

The studies described above explore FA presence and variation in one or two primate taxa to explore broader questions about the mechanisms by which FA is produced, but it is still unclear how FA magnitude is patterned across the cranium. While using FA to study morphological integration has become popular in the last few decades (e.g., Klingenberg, **2003a, 2003b, 2008**; Singh et al., **2012**), studies assessing variation in magnitude of FA across the cranium are rare. The amount and pattern of FA distributed across the cranium can provide clues to the factors contributing to FA such as the influence of bone turnover (Hallgrímsson, **1993**) or ossification patterns. Further, composite FA indices are the recommended measure for evaluating the amount of FA in a sample (Leung et al., **2000**), and the contribution of various cranial regions to these indices is relevant when selecting traits to include in a study.

Cranial development may help elucidate patterns of FA. Bones of the cranium develop via two ossification pathways: endochondral and intramembranous ossification. The cranial base forms primarily by endochondral ossification, while the remaining bones of the face (e.g., zygomatic and maxilla) and the cranial vault (e.g., parietal and frontal) form via intramembranous ossification (Scheuer & Black, **2000**). Endochondral ossification is a process where bone is formed from a cartilaginous template (Jin et al., **2016**) while intramembranous ossification occurs from mesenchymal cells that create ossification centers that differentiate into osteoblasts that then produce bone (Mackie et al., **2008**). Further, the cranial base is the first area of the cranium to fuse, followed by the vault and then the face (Scheuer & Black, **2000**). These processes and patterns of fusion in the cranium can offer a clue as to what we might see in patterns of FA across the cranium.

The cartilaginous template that is a precursor to endochondrally ossified bones of the cranium forms early in development. In humans, this template is formed in the first trimester of pregnancy and forms

similarly early in other mammals (Javed et al., **2010**). This early template formation may leave less room for changes during the remaining period of development, so we may see less FA and FA variance in regions forming via endochondral ossification than those that ossify intramembranously. This idea is supported by the relatively high narrow-sense heritability estimates found in the basicranium, which indicate tighter genetic control of this region (Joganic et al., **2012**). If FA accrues over ontogeny as Hallgrímsson (**1999**) suggests, then we might see higher FA in cranial regions that fuse later in development than others (e.g., face), either as a result of decreased developmental stability in these regions or perhaps functional asymmetry related to increased mechanical loading. An alternative outcome could be that all cranial regions exhibit relatively equal levels of FA, meaning that FA is not likely related to ossification pattern or level of genetic control.

Previous studies of primate crania found that the masticatory region is generally more variable than other cranial regions but that it equally reflects phylogenetic relationships compared to other regions, indicating that there may be no genetic difference in control of masticatory versus other regions (von Cramon-Taubadel, **2009, 2011**; von Cramon-Taubadel & Smith, **2012**). Additionally, the patterns of magnitude in FA across landmarks can point to more or less useful landmarks for analyzing FA in primates. Landmarks that exhibit high variation in magnitudes of FA will be most useful in studies of FA, whereas landmarks with little variation in FA can be excluded in future analyses.

1.3 Research goals and hypotheses

Here, we analyze FA magnitude between taxa and FA variation across the cranium to offer new insights on craniofacial evolution that may provide clues to the factors influencing developmental instability in primates. This study offers an initial, preliminary investigation into FA levels and the amount of variation in the crania of western lowland gorillas (*G. gorilla gorilla*), central chimpanzees (*P. troglodytes troglodytes*), and crab-eating or long-tailed macaques (*M. fascicularis fascicularis*) using three-dimensional geometric morphometric techniques. This study offers an initial, preliminary investigation into FA levels and the amount of variation in FA across the primate cranium. These data can offer new insights on craniofacial evolution and may provide clues to the factors influencing developmental stability in primates. This investigation is the first cross-species study of FA magnitude and FA variance in nonhuman primates.

We specifically address two research questions regarding (1) how total cranial FA is patterned across primate species and (2) how FA is patterned regionally across the cranium. First, we investigate the magnitude and variance of total cranial FA in *Gorilla*, *Pan*, and *Macaca*. We expect that more closely related species will exhibit similar levels of cranial FA (i.e., *Gorilla* and *Pan* should exhibit more similar magnitudes of FA than they do to *Macaca*). Second, we anticipate that variation in FA across the cranium will be patterned in relation to phylogeny, bone development, and function. Cranial regions with higher heritability should align more closely with phylogenetic relationships. Therefore, the cranial base in *Gorilla* and *Pan* should exhibit closer levels of FA variance than in *Macaca*, whereas the face and vault may not exhibit any particular relationship. We expect that if genetic factors are the primary influence over developmental stability, then cranial regions that develop and cease growth earlier (and are thus argued to be more tightly genetically controlled) will show lower levels of FA variance (Joganic et al., **2012**). In comparison, cranial regions that take longer to develop (i.e., more time to accumulate random deviations) and may also be subject to increased mechanical loading and environmental

perturbation will exhibit relatively higher levels of FA variance. Thus, we expect that the cranial base will exhibit lower levels of FA variance than the cranial vault or face because it ceases growth before the vault and face regions.

2 MATERIALS AND METHODS

2.1 Data collection

We measured FA in a wild-caught sample of *G. gorilla gorilla* ($n = 22F, 22M$), *P. troglodytes troglodytes* ($n = 17F, 20M$), and *M. fascicularis fascicularis* ($n = 19F, 20M$; Table **S1**). Only adult specimens were included (as determined by the third molar eruption) and individuals with obvious pathologies and missing or broken bone were excluded (Jung & von Cramon-Taubadel, **2018**). These gorilla and chimpanzee species live sympatrically in Western Africa, while the long-tailed macaque is native to Southeastern Asia. These sympatric ape species were chosen in an attempt to control for the physiological effects differing environments may induce, and long-tailed macaques were chosen as an outgroup. Additionally, only one subspecies of *Gorilla*, *Pan*, and *Macaca* were used in an effort to limit variation that is a result of differences at the subspecies level.

Three-dimensional (3D) scans of primate crania were obtained from colleagues or in person (Table **S1**). Twenty-one *G. gorilla gorilla* and *P. troglodytes troglodytes* 3D surface models were created by M. Tocheri from CT scans he generated at the National Museum of Natural History. 3D scan data for *M. fascicularis fascicularis* were generated using an HDI 120 blue LED scanner at the Field Museum by CET. This same scanner was used to collect 3D scan data for the majority of the *Gorilla* and *Pan* specimens from the Cleveland Museum of Natural History by ANR. All scans taken with the HDI 120 blue LED scanner were processed using FlexScan (LMI Technologies) and Geomagic Studio (3D Systems, Inc.) software. The surface models from M. Tocheri were processed in Geomagic Studio software. The differences multiple scanning methodologies create are negligible in 3D geometric morphometric studies (Robinson & Terhune, **2017**).

For all specimens, 74 fixed 3D landmarks were placed across the cranium by ANR in three separate trials using Landmark Editor (Figure **1**; Wiley et al., **2005**). Multiple trials are required for studies of FA because error is incorporated into the statistical models used for data analysis and FA is a subtle phenomenon where noise can outweigh the signal (Klingenberg, 2015; Palmer & Strobeck, **1986**). Increasing trial number allows for a better characterization of FA in the sample (Graham et al., **2010**; Klingenberg, 2015). Landmarks included eight midline landmarks and 33 bilateral landmark pairs across the face, base, and vault of the cranium (Table **1**). Landmarking errors were detected in the MorphoJ software (Klingenberg, **2011**) using the “find outliers” function and re-digitized if gross errors such as mislabeling of landmarks or landmark misplacement/reversal were obvious.

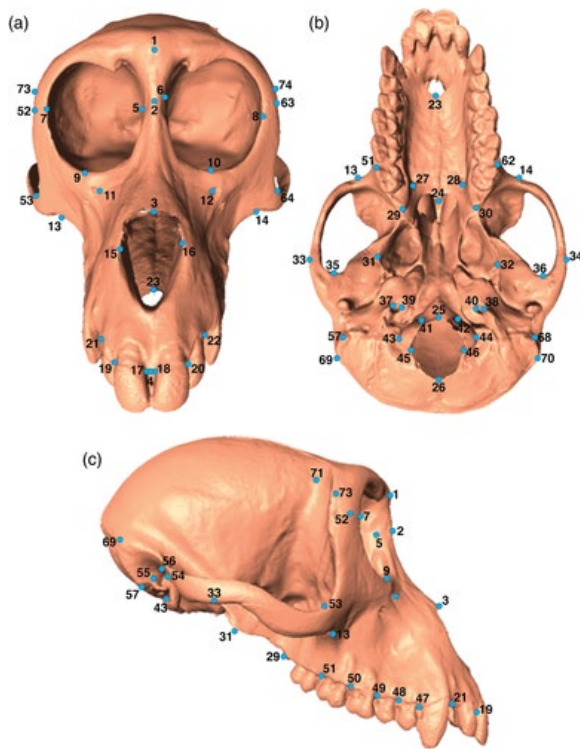


FIGURE 1 Visualization of the 74 landmarks used in this study on a *Macaca fascicularis fascicularis* specimen (FMNH 66332). (a) Anterior view (b) inferior view (c) right lateral view. Refer to Table 1 for landmark definitions

TABLE 1. Landmarks used in this study

Landmark	Midline/bilateral	Location	Description
1	Midline	Vault	Most anterior midline point on the frontal bone
2	Midline	Face	Most narrow and anterior aspect of nasal bones between the orbits (inferior to nasion)
3	Midline	Face	Most inferior and middle extent of nasal bone juncture
4	Midline	Face	Most superior fused point on the intermaxillary suture
5, 6	Bilateral	Face	Most medial point along the supraorbital margin
7, 8	Bilateral	Face	Most lateral point along the orbital margin
9, 10	Bilateral	Face	Most inferior point along the lower orbital margin (Orbitale)
11, 12	Bilateral	Face	Superior margin of the infraorbital foramen (in the case of a secondary infraorbital foramen, score the most medial foramen)
13, 14	Bilateral	Face	The most medial/inferior point of the masseter muscle attachment
15, 16	Bilateral	Face	The most lateral point on the nasal aperture taken perpendicular to the nasal height (Alare)
17, 18	Bilateral	Face	Most anterior and inferior point along the alveolar border between central incisors
19, 20	Bilateral	Face	Central point between alveoli of central and lateral incisors

21, 22	Bilateral	Face	Middle point on inferior margin of alveoli between the canine and lateral incisor
23	Midline	Face	The most posterior, inferior point on the incisive fossa (most posterior, inferior point between incisive foramina when there are two)
24	Midline	Face	Midline point on interpalatal suture corresponding to the deepest point of notches at the rear of the palate
25	Midline	Base	The point where the anterior margin of the foramen magnum intersects the midsagittal plane
26	Midline	Base	The point where the posterior margin of the foramen magnum intersects the midsagittal plane
27, 28	Bilateral	Face	The most posterior, inferior point on the greater palatine foramen
29, 30	Bilateral	Face	The point on the inferior surface of the maxilla that denotes the most posterior point of the alveolar process
31, 32	Bilateral	Base	Most anterior and inferior point on the hamulus
33, 34	Bilateral	Face	The most lateral point on the surface of the zygomatic arch
35, 36	Bilateral	Vault	The most posterior point on the temporal fossa
37, 38	Bilateral	Base	The most lateral point on the carotid canal
39, 40	Bilateral	Base	The most medial point on the carotid canal
41, 42	Bilateral	Base	The most anterior point on the occipital condyle
43, 44	Bilateral	Base	The most lateral point on the occipital condyle
45, 46	Bilateral	Base	The most lateral point on the margin of the foramen magnum and posterior to occipital condyle
47, 58	Bilateral	Face	The most anterior point on the alveolus of the third premolar
48, 59	Bilateral	Face	The most anterior point on the alveolus of the fourth premolar
49, 60	Bilateral	Face	The most anterior point on the alveolus of the first molar
50, 61	Bilateral	Face	The most anterior point on the alveolus of the second molar
51, 62	Bilateral	Face	The most anterior point on the alveolus of the third molar
52, 63	Bilateral	Face	The most lateral antero-posterior midpoint on the zygomaticofrontal suture
53, 64	Bilateral	Face	Deepest point in the anterior notch of zygomatic bone (Jugale)
54, 65	Bilateral	Vault	The most anterior superior–inferior midpoint on the margin of the external auditory meatus
55, 66	Bilateral	Vault	The most posterior superior–inferior midpoint on the margin of the external auditory meatus
56, 67	Bilateral	Vault	The most superior point on the margin of the external auditory meatus
57, 68	Bilateral	Vault	The most lateral, inferior point on the mastoid process

69, 70	Bilateral	Vault	The most lateral point on the process created by the mastoid and temporal bone
71, 72	Bilateral	Vault	The most lateral point on the most medial inflection of the cranial vault behind the browridge
73, 74	Bilateral	Vault	The most lateral point on the frontal bone (brow ridge)

Note: Landmark number corresponds to the landmark order used to place landmarks on specimens. Midline landmarks are a single landmark while bilateral landmarks have a landmark placed on both the right and left sides of the specimen. Location categorizes landmarks by region (face, cranial base, or cranial vault).

2.2 Data analysis

Crania were analyzed in MorphoJ software (Klingenberg, **2011**) by first performing a generalized Procrustes fit (GPA) to superimpose the landmark configurations separately for each species group. Crania have object symmetry, meaning the right and left side of each cranium is a part of the symmetric whole, and the axis of symmetry passes through each cranium (Klingenberg, 2015). When configurations with object symmetry are analyzed via GPA in MorphoJ, GPA is performed on both the original and reflected landmark configurations for all specimens; this analysis produces both a symmetric and an asymmetric component of shape (Klingenberg et al., **2002**). The symmetric component of shape consists of the average or consensus shape calculated from the original and reflected landmarks in the configuration. This component is often used in studies of shape variation where asymmetry might confound results or in studies that need to reconstruct missing landmarks. The asymmetric component of shape, which is our interest here, represents the differences between the original and mirrored landmark configurations for each specimen. To assess the significance of FA in our sample, we performed a Procrustes analysis of variance (ANOVA) on the asymmetric component of shape for each species (Klingenberg & McIntyre, **1998**). This ANOVA model used the individual (fixed), side (fixed), and trial error (random) as main effects to understand how the right and left side landmarks and individual landmark configurations relate to each other and further compared the sizes of the right and left sides of the landmark configurations to test the difference between these two groups (Klingenberg & McIntyre, **1998**; Palmer, **1994**; Palmer & Strobeck, **1986**). The Procrustes ANOVA determines statistical significance of the directional (side) and fluctuating (individual \times side) asymmetry present in the sample tested, quantifies the signal-to-noise (error) ratio in the sample for FA, and provides a Procrustes FA score for each specimen (Klingenberg & Monteiro, **2005**). The signal-to-noise ratio provides a measure of how easily FA is detectable when compared to the error between landmarking trials in the sample. This ratio is the F value for the individual \times side (or FA) effect and the error effect, which is calculated by dividing the mean square of the individual \times side (FA) effect by the mean square of the error effect. From these Procrustes ANOVA results, we calculated the percent each factor contributed to the overall variation by dividing the sum of squares for each factor by the total of all sum of squares factors added together (Gómez-Robles et al., **2013**). Lastly, we exported the individual Procrustes FA scores for each specimen from the Procrustes ANOVA results in MorphoJ for further analysis using other software (**Table S2**).

We ran the above analyses three slightly different ways: (1) with a separate GPA and separate Procrustes ANOVA for each species, (2) a single GPA and single Procrustes ANOVA for all specimens, and (3) a separate GPA for each species but then subdivided the specimens by species without

performing a new GPA and performed a separate Procrustes ANOVA on each species. While the values differed slightly, the same overall trends were found for each of the three sets analyses. The methods and results of analysis (1) are reported here.

Descriptive statistics such as mean, standard error, and variance were calculated for the Procrustes FA scores in Microsoft Excel for each species and for males and females within each species. We specifically examined two measures of FA to address our first research question: the magnitude of differences in the FA scores between sexes and among taxa, and levels of variance in FA scores between sexes and among taxa. The Procrustes FA values were visualized via box plots and further analyzed in R to examine differences between taxa and sexes (R Core Team, **2017**). To test for differences in FA scores among taxa and sexes and evaluate the interaction between these two factors, a two-way ANOVA was performed on the FA scores with the taxon, sex, and the interaction between the two as the main effects. Then, a Tukey Honest Significant Differences (HSD) post-hoc comparison of groups was run on taxon groups and sex groups within each taxon to determine which groups were significantly different from one another.

To examine variation in FA across the cranium, we analyzed how variable FA was in individual landmarks and how they might contribute to overall FA. First, we extracted the FA component coordinates from the *bilat.symmetry* function in the *geomorph* package in R (Adams et al., 2020). These coordinates represent the asymmetry component around the mean asymmetry (directional asymmetry) for each landmark on each specimen. Then, for each landmark, we calculated the landmark mean for the entire sample (mean of coordinate *x*, mean of coordinate *y*, and mean of coordinate *z*). Next, for each landmark, we calculated the distance from that landmark in each individual to the grand mean of that landmark across all individuals using the following equation

$$\sqrt{(x_n - x_{\text{mean}})^2 + (y_n - y_{\text{mean}})^2 + (z_n - z_{\text{mean}})^2},$$

where x_n , y_n , and z_n is the coordinate of the landmark for any given specimen and x_{mean} , y_{mean} , and z_{mean} is the mean landmark coordinate for all specimens. Lastly, from these landmark distances, we then calculated the average distance of all specimens to the grand mean for each landmark and the standard deviation for each average distance. In this instance, the average distance for each landmark tells us the magnitude of asymmetry at each landmark and the variance in the landmark around the grand mean. After doing this analysis with all specimens pooled, we divided the specimens by taxon and performed the analysis on each taxon separately.

After calculating the variation in FA at each landmark, we tested the difference in FA variance between cranial regions (face, base, and vault) in the pooled specimens and for each species individually using Kruskal–Wallis rank sum tests. We also tested the difference between species within each cranial region. Further, we performed the analyses described above on a subset of the eight landmarks exhibiting the most variation in FA. Then, heatmaps of variation magnitudes were plotted across the cranium using the *landvR* and *geomorph* packages in R (Adams et al., **2020**; Guillaume & Weisbecker, **2019**). To do this, we found the specimen closest to the mean shape in our sample, the coordinates of the specimen that represented the mean shape in our sample, and then warped the mesh to those coordinates. We then colored the landmarks across the cranium by the amount of

variation at that landmark (i.e., red represents the most variation and yellow represents the least variation for a landmark).

3 RESULTS

3.1 Is FA present in the sample?

The initial Procrustes ANOVA on the asymmetric component of shape for each species demonstrated that the side effect (directional asymmetry) and the individual \times side interaction (FA) were both statistically significant ($p < 0.0001$ for both) in every group, meaning that both directional asymmetry and FA were present in each species in the sample (Table 2). Across species, the individual effect was statistically significant and contributed the most variation to the sample (80%–85%; Table 2).

Directional asymmetry was present across species but contributed very little to the total variation in the sample. FA was consistently from 6% to 10% of the total variation in the sample across species groups, while error varied but was particularly high for *Pan*. Though error contributed more to the total variance than FA in *Gorilla* and *Pan*, the signal to noise ratio across species in this sample showed that the effect was at least two times greater than the error in each species (*Gorilla* = 4.14, *Pan* = 2.31, *Macaca* = 4.98; Table 2).

TABLE 2. Results of Procrustes ANOVA on the asymmetric component of shape for each taxon and two-way ANOVA on FA scores

ANOVA type	Effects	df	Sum of Sq	Mean Sq	F value	Pr(>F)	% Var (%)
Procrustes ANOVA	Individual	4773	0.558	1.17e-4	10.88	<0.0001*	84.64
<i>Gorilla</i>	Side (DA)	104	0.004	3.86e-6	3.59	<0.0001*	0.61
	Individual \times side (FA)	4472	0.048	1.07e-6	4.14	<0.0001*	7.29
	Error	18,920	0.049	2.59e-6	—	—	7.45
Procrustes ANOVA	Individual	3996	0.337	8.43e-5	11.17	<0.0001*	80.24
<i>Pan</i>	Side (DA)	104	0.003	2.65e-5	3.51	<0.0001*	0.66
	Individual \times side (FA)	3744	0.028	7.55e-6	2.31	<0.0001*	6.73
	Error	15,910	0.052	3.26e-6	—	—	12.37
Procrustes ANOVA	Individual	4218	0.379	8.99e-5	9.02	<0.0001*	82.48
<i>Macaca</i>	Side (DA)	104	0.008	7.31e-5	7.34	<0.0001*	1.65
	Individual \times side (FA)	3952	0.039	9.96e-6	4.98	<0.0001*	8.56
	Error	16,770	0.033	2.00e-6	—	—	7.30
FA scores ANOVA	Taxon	2	0.0001634	8.17e-05	5.42	0.0056*	—
	Sex	1	0.0000006	5.80e-07	0.04	0.8444	—

	Taxon × Sex	2	0.0001695	8.47e-05	5.62	0.0047*	—
	Residuals	114	0.0017181	1.51e-05	—	—	—

Note: The percent each factor contributes to the overall variation is included in the last column for the Procrustes ANOVAs.

Abbreviations: ANOVA, analysis of variance; DA, directional asymmetry; FA, fluctuating asymmetry.

* Statistical significance below the $\alpha = 0.05$ level.

3.2 Does the magnitude of FA differ among taxa and sexes?

The two-way ANOVA on the Procrustes FA values (Table 2) exported from MorphoJ demonstrated that taxa had significantly different FA levels ($p = 0.006$), sexes were not significantly different from one another when pooled across species ($p = 0.844$), and the interaction between taxon and sex was significant ($p = 0.0047$) meaning that species showed different magnitudes of FA by sex. The interaction plot for the two-way ANOVA showed that the interaction between taxon and sex mostly applied to *Gorilla* and *Macaca* but in opposite directions, while FA in *Pan* remains similar between the two sexes (Figure 2). The differences between sexes in *Gorilla* were significant ($p = 0.026$), while differences in *Macaca* only approached significance ($p = 0.063$). There was no statistically significant difference between sexes in *Pan* ($p = 0.814$). Visualization of the data (Figure 3, Table 3) indicated that *Gorilla* had the highest mean FA (0.0186), with female gorillas tending to have lower FA than male gorillas. *Macaca* had similarly high levels of mean FA (0.0178), but female macaques tended to have higher FA than male macaques. *Pan* had the lowest mean FA (0.0158), with the mean values for male and female chimps nearly identical. The Tukey's HSD post-hoc comparisons showed that significant differences between taxa were driven by *Pan* and *Gorilla* ($p = 0.004$) and confirmed that there was no significant difference between sexes when pooled across species. Additionally, the taxon × sex interaction was driven by differences between male *Gorilla* and female *Pan* ($p = 0.01$), male *Macaca* and male *Gorilla* ($p = 0.04$), and male *Pan* and male *Gorilla* ($p = 0.005$).

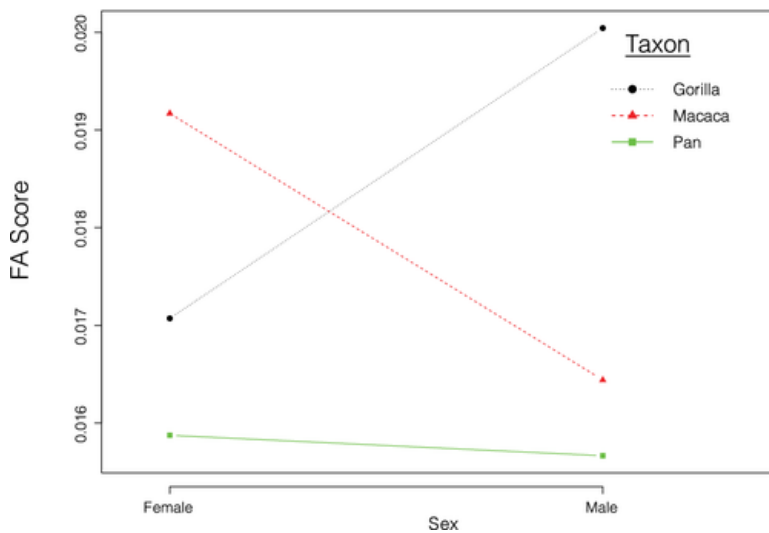


FIGURE 2 Interaction plot for two-way ANOVA showing the mean FA value for each sex in each species under study. ANOVA, analysis of variance; FA, fluctuating asymmetry

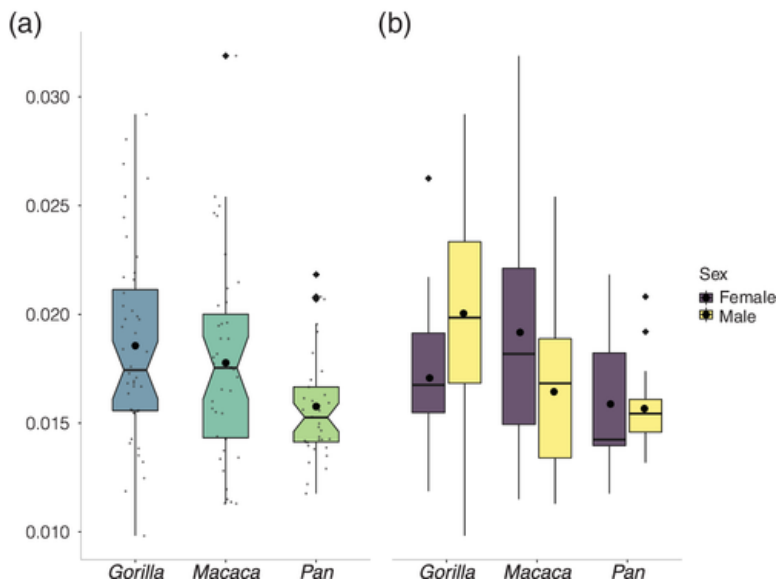


FIGURE 3 (a) Boxplot showing FA value distributions by species with the individual values overlying the plots. The large black circle represents the mean value for each species. The black diamonds represent outliers in the data. The notches in the boxes help compare groups. Notches that do not overlap suggest significantly different median values. (b) Boxplot showing the distribution of FA values in each sex for each species in the study. The large black circle represents the mean for each sex within each species. The lines through the colored boxes show the median values. The colored boxes represent the second and third quartile (i.e., 25th–75th percentile), and the whiskers represent the first and fourth quartiles (i.e., 1st–25th percentile and 75th–100th percentile). The smaller points in the plot represent the spread of the data within each box. FA, fluctuating asymmetry

TABLE 3. Descriptive statistics of FA scores with sample size (n), mean, range, variance (σ^2), and standard error (SE) for each species

Group	n	Mean	Range	σ^2	SE
<i>Gorilla</i>	44	0.019	0.019	1.99e-05	3.00e-06
Female	22	0.017	0.014	1.13e-05	2.40e-06
Male	22	0.020	0.019	2.49e-05	5.31e-06
<i>Pan</i>	37	0.016	0.010	6.35e-06	1.04e-06
Female	17	0.016	0.010	1.02e-05	2.49e-06
Male	20	0.016	0.008	3.38e-06	7.56e-07
<i>Macaca</i>	39	0.018	0.021	2.11e-05	3.38e-06
Female	19	0.019	0.020	2.66e-05	6.11e-06
Male	20	0.016	0.014	1.32e-05	2.95e-06

Abbreviation: FA, fluctuating asymmetry.

3.3 Does variance in FA differ among taxa and sexes?

Variance in FA levels followed a similar trend as mean FA scores among these taxa (Table 3). *Pan* exhibited the lowest variance in FA level ($\sigma^2 = 0.0000063$), while *Gorilla* and *Macaca* were higher ($\sigma^2 = 0.00002$ for both taxa). The differences in variance between *Pan* and both *Gorilla* and *Macaca* were statistically significant ($p = 0.0003$ and $p = 0.0002$,

respectively), but the difference in variance between *Gorilla* and *Macaca* was not statistically significant ($p = 0.4$). Differences in the variance of FA by sex within each taxon existed as well. Male gorillas exhibited higher variance in FA than female gorillas ($p = 0.04$), female chimpanzees exhibited higher variance in FA than males ($p = 0.01$), and female macaques did not exhibit a statistically significant difference in variance from male macaques ($p = 0.07$) (Table 3, Figure 3).

3.4 Does FA variance differ between cranial regions?

Both when specimens were pooled and when species were analyzed separately, no cranial region differed from the others in FA variance ($p > 0.05$ for all). Only cranial regions in *Gorilla* approached significance ($p = 0.06$), which was driven by near-significance of differences in the cranial base and vault regions. Additionally, there was no difference in FA variance in cranial regions between species ($p > 0.05$ for all). Of the 33 bilateral landmarks that captured information about asymmetry in these specimens, eight landmarks varied around the mean FA landmark by 0.004 mm or more when all the specimens were pooled (Table 4). These eight landmarks represented the top 10% of the 74 landmarks used in this study with the most variation in FA. These landmarks were located across the cranium without any clear pattern by region (Figure 4). When analyzed by taxa, many of the most variable landmarks for FA were similar to those when specimens are pooled (Table 4). The landmarks that were among the most variable for all taxa (whether analyzed individually or pooled) were the most lateral point on the zygomatic arch, the most inferior point on the mastoid process, the most lateral point on the cranial vault when viewed posteriorly, the pterygoid hamulus, and aspects of the orbit (most lateral, superior, or inferior point). When analyzed separately, the subset of eight landmarks with the most variation in FA had an increased mean FA magnitude and variance across all groups and sexes. The trends in significance were similar to analyses with the full landmark dataset with FA magnitude in *Pan* significantly different from *Gorilla* and *Macaca*. However, *Gorilla* and *Macaca* were not significantly different from one another ($p < 0.001$ for all significant comparisons; Table S3), and there was no significant difference in FA magnitude between sexes in all taxa. Further, the percent each effect in the Procrustes ANOVA contributed to the sample variation in asymmetric shape was quite different for *Macaca*, where FA nearly doubled its contribution (Table S4).

TABLE 4. Summary of landmark variation observed for each species

Landmark number	Distance from mean landmark	Standard deviation	Description
<i>Pooled specimens</i>			
33/34	0.0061	0.0048	The most lateral point on the surface of the zygomatic arch
69/70	0.0056	0.0049	The most lateral point on the process created by the mastoid and temporal bone
57/68	0.0050	0.0027	The most lateral, inferior point on the mastoid process
5/6	0.0047	0.0035	Most medial point along supraorbital margin
31/32	0.0046	0.0027	Most anterior and inferior point on the hamulus

71/72	0.0045	0.0029	The most lateral point on the most medial inflection of the cranial vault behind the brow ridge (postorbital constriction)
7/8	0.0041	0.0023	Most lateral point along the orbital margin
9/10	0.0041	0.0037	Most inferior point along the lower orbital margin (Orbitale)
<i>Gorilla</i>			
69/70	0.0074	0.0064	The most lateral point on the process created by the mastoid and temporal bone
71/72	0.0058	0.0038	The most lateral point on the most medial inflection of the cranial vault behind the brow ridge (postorbital constriction)
57/68	0.0049	0.0022	The most lateral, inferior point on the mastoid process
31/32	0.0047	0.0027	Most anterior and inferior point on the hamulus
33/34	0.0046	0.0046	The most lateral point on the surface of the zygomatic arch
7/8	0.0041	0.0024	Most lateral point along the orbital margin
73/74	0.0041	0.0031	The most lateral point on the frontal bone (brow ridge)
9/10	0.0041	0.0046	Most inferior point along the lower orbital margin (Orbitale)
<i>Pan</i>			
33/34	0.0054	0.0035	The most lateral point on the surface of the zygomatic arch
31/32	0.0047	0.0027	Most anterior and inferior point on the hamulus
52/63	0.0044	0.0037	
69/70	0.0044	0.0024	The most lateral point on the process created by the mastoid and temporal bone
57/68	0.0043	0.0024	The most lateral, inferior point on the mastoid process
5/6	0.0042	0.0027	Most medial point along the supraorbital margin
7/8	0.0041	0.0022	Most lateral point along the orbital margin
11/12	0.0035	0.0025	Superior margin of the infraorbital foramen (in the case of a secondary infraorbital foramen, score the most medial foramen)
<i>Macaca</i>			
33/34	0.0076	0.0055	The most lateral point on the surface of the zygomatic arch
5/6	0.0058	0.0036	Most medial point along supraorbital margin
57/68	0.0051	0.0027	The most lateral, inferior point on the mastoid process
69/70	0.0048	0.0038	The most lateral point on the process created by the mastoid and temporal bone

9/10	0.0047	0.0038	Most inferior point along lower orbital margin (Orbitale)
31/32	0.0044	0.0025	Most anterior and inferior point on the hamulus
19/20	0.0042	0.0034	Central point between alveoli of central and lateral incisors
55/66	0.0042	0.0054	The most posterior superior–inferior midpoint on the margin of the external auditory meatus

Note: For each group, the top eight mean distances from the mean landmark for FA. Component landmarks are provided.

Abbreviation: FA, fluctuating asymmetry.

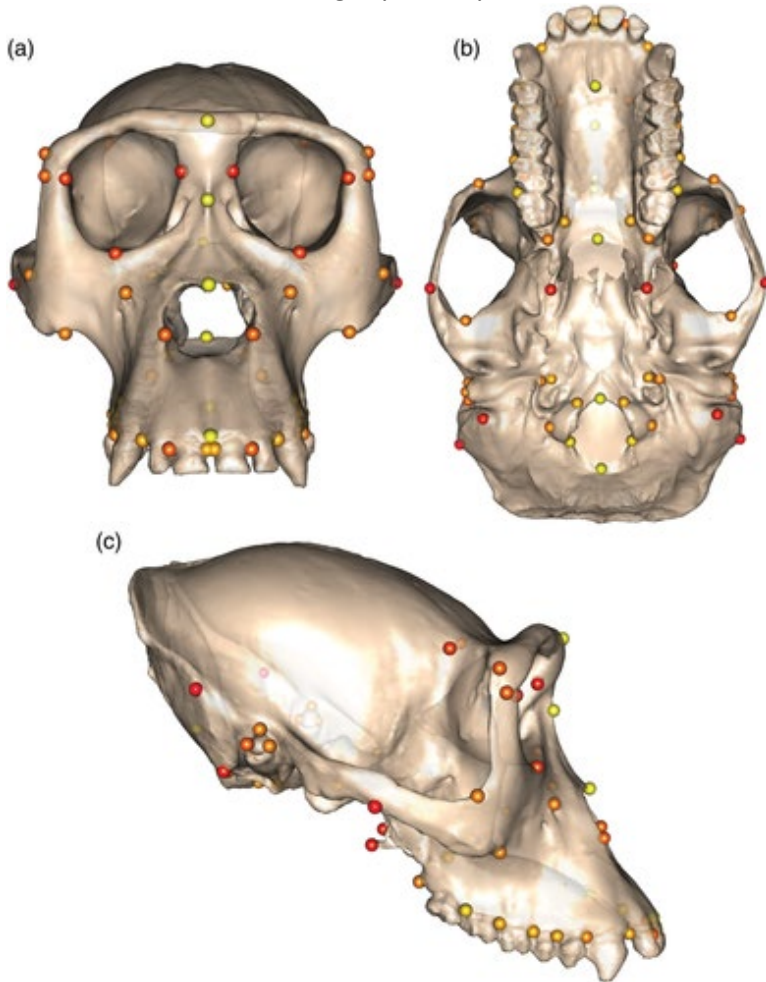


FIGURE 4 Variation in FA by landmark for the entire sample in this study with colors indicating the amount of variation at that landmark on a spectrum of red to yellow. A red orb represents the most variation in FA at that landmark and a yellow orb represents the least amount of variation in FA at that landmark with a range of colors in between. These landmarks represent the FA variation in the entire sample in this study but are projected on a female *Gorilla gorilla gorilla* specimen for visualization (CMNH 1798). (a) Anterior view (b) inferior view (c) right lateral view. FA, fluctuating asymmetry

4 DISCUSSION

The goal of this study was to learn more about the magnitude and variation of FA across primate groups and the primate cranium. We tested the difference in magnitude and variance of FA in this

sample between three primate taxa and the variation in FA across the cranium (face, base, and vault). We expected that *Gorilla* and *Pan* would exhibit closer magnitudes of total cranial FA due to their closer relationship to one another than to *Macaca*, and we expected that the cranial base would exhibit this same relationship in FA variance. We also anticipated that the FA variance in the cranial base would be lower than in the face or vault due to the higher heritability and tighter genetic control, the early cessation of growth, and the lower mechanical force from mastication in this area. Our results do not support these hypotheses. While the observed variation in FA matches the pattern of FA magnitude between taxa, gorillas and macaques have more similar magnitudes of FA and variation in FA than chimpanzees (i.e., both magnitude and variation in FA is higher in gorillas and macaques than in chimpanzees). The FA variance in cranial regions is not significantly different among the primate taxa in this study nor is there a difference in FA variance of cranial region within taxa. Additionally, variation in FA at each landmark appears to be random.

4.1 FA across primate taxa

Our results indicate that the *Gorilla* and *Macaca* populations sampled here exhibit similar magnitudes of FA, while the *Pan* population exhibits a lower magnitude of FA. These findings between taxa are significantly different. Differences between sexes were not statistically significant when data were pooled across species, but the interaction effect between sex and species was significant. This result does not have a clear pattern as the sex exhibiting more FA changes from species to species. These findings do not support our hypothesis that more closely related species will exhibit similar levels of FA. Rather, this finding follows what would be expected if FA is influenced more heavily by environmental rather than genetic factors. However, we cannot draw conclusions on cross-species comparisons for primates more generally because this preliminary study includes only three species.

One possible explanation for the trend of FA magnitude seen here is growth rate rather than growth duration. In a comparison in the height of production rate, or growth constant, in 36 sex-pooled primate species, Mumby and Vinicius (2008) found that crab-eating or long-tailed macaques (*M. fascicularis*) and gorillas (*G. gorilla*) grow faster than chimpanzees (*P. troglodytes*). The chimpanzee growth constant (calculated from growth curves for these species) is 0.28, while it is 0.39 in gorillas and 0.36 in macaques. We observed the same pattern here for FA magnitude that we see for growth constants at a species level in chimpanzees, gorillas, and macaques; that is, chimpanzees show lower levels of FA than gorillas and macaques. However, growth rate as a significant predictor of FA is only supported in the *Gorilla* taxon where males have higher growth rates (Leigh, 1996) and higher levels of FA. This trend was not followed in *Macaca* and *Pan* where sexes showed no significant difference in FA magnitude despite having differing growth rates (Leigh, 1996).

The variation in the magnitude of FA in these taxa show a slight difference in pattern than the mean values. *Macaca* has the largest variation of FA magnitude followed closely by *Gorilla*, while *Pan* is quite constrained in comparison. Unfortunately, literature on variation in growth rate or morphological variability related to growth rate between sexes and/or between the primate species analyzed here is lacking, so no meaningful comparisons of the two can be offered. The lower magnitude of FA and low variance of FA magnitude in central chimpanzees suggests that the sample from this taxon experiences the least variation in developmental disturbance and/or has the best ability to buffer against the instability of the species considered in this study. Alternatively, it is possible that this sample of central

chimpanzees experienced less stress during development than either the sample of macaques or gorillas. Unfortunately, measurements for FA are nonspecific and do not provide information about what processes or life experiences led to levels of FA seen in individuals, and in many circumstances, stress increases levels of FA (Hoffman & Woods, **2003**). Rather than being a product of growth rate or genetics, the observed pattern of FA levels in these primate species are more likely to be due to differences in stress experiences between these groups (e.g., social status, malnutrition, and parasite load). If that is the case, it is unclear why the central chimpanzees in this sample would experience less stress than the sympatric western lowland gorillas or the macaques in Southeast Asia, but the contribution of stress to FA level cannot be discounted. Further, determining the underlying cause of lower levels of FA in *Pan* is extremely difficult. As stated, both increased developmental stability or low levels of stress, or even a combination of the two, could result in the low magnitude of FA in *Pan*. No clear solution is offered for this paradox, as changes in the degree of developmental stability could be occurring, behavioral accommodations could be reducing stress levels, and/or individuals could be living in a less stressful environment.

4.2 FA across the primate cranium

Our results for FA variance indicate that there is no difference between cranial regions within each species nor between the same cranial region across different species, which matches results seen in humans (Jung & von Cramon-Taubadel, **2018**). We see no patterning in FA variance by bone development type or phylogenetic relationship. The variation of FA by landmark also shows no clear patterning. While these results do not provide any information about the processes that result in developmental stability, they do suggest that some landmarks may be more useful than others for measuring FA in primates. Landmarks with more variation in FA are more informative for comparing FA among individuals and taxa, while those with less variation offer little information for these types of inquiries. Landmarks that appear to be less useful for examining FA are those on the medial parts of the occipital condyles, the posterior aspect of the temporal fossa, the posterior alveolar process, and the alveolus between the premolars and molars. The most useful landmarks for assessing FA appear to be those surrounding the orbits, on the lateral zygomatic arch, the posterior external auditory meatus, and the lateral aspect of the posterior vault. These results offer regional foci that may be useful for further investigation of FA in the primate cranium. It is important to note that all of the landmarks in our sample are fixed landmarks, and many of the landmarks with the most variation are found at geometric extremes on the cranium, or type III landmarks (i.e., the most lateral point on the zygomatic arch when the cranium is viewed in the inferior position). Each landmark configuration in this sample was collected three times to reduce both observer error that may contribute to the variation in FA magnitude seen, but these geometric extremes are not always entirely homologous and may therefore inflate the observed values.

4.3 Potential application to primate conservation

In addition to providing information about the generation or reduction of variation, studies of FA, and by proxy developmental instability, are also a potential avenue for informing primate conservation efforts. If individuals in a particular species exhibit more asymmetry (and therefore lower developmental stability) than another, that species may have more urgent conservation needs than those with greater developmental stability (Delgado-Acevedo & Restrepo, **2008**). In this respect, our

results suggest that gorillas may require more conservation intervention than chimpanzees, or at least they might have at the time these samples were collected. This matches the assessment of the International Union for Conservation of Nature and Natural Resources Red List that designates western lowland gorillas as critically endangered and central chimpanzees in a slightly less severe endangered category, though both taxa are in dire need of conservation efforts.

The differences observed could reflect reduced ability to buffer against environmental stress in western lowland gorillas as indicated by higher levels of FA when compared to central chimpanzees. Western lowland gorillas (*G. gorilla gorilla*) and central chimpanzees (*P. troglodytes troglodytes*) both primarily eat fruits in their central African habitats, but gorillas are able to “fallback” on a folivorous diet when fruits are scarce (Marshall & Wrangham, 2007). Further, studies have shown that chimpanzees are more endangered by environmental degradation (e.g., logging) than gorillas in central Africa (Morgan & Sanz, 2007). Our results indicate that populations with more stable resources exhibit higher levels of FA as Emlen et al. (1993) suggested, meaning that they may evolve lower levels of developmental stability over time and respond more unfavorably to environmental stresses than their counterparts who experience higher levels of stress more often. This may be true of *M. fascicularis*, but further research is required to understand the higher magnitude of FA in this group. Samples from sympatric populations offer great potential for examining FA as a proxy for environmental stress and can be used as an additional justification for conservation categories and conservation efforts in the future.

Any potential for FA to apply to primate conservation will require further research before implementation. Here, we have specimens from the same subspecies but not necessarily the same locality nor the same time period. Population-specific studies are needed to further understand the relationship between FA and environmental variables because often these stresses are particular to the area in which a population lives. Previous work has examined “fitness” in relation to FA in a number of species, including humans (see review in Møller, 1997). One of these fitness measurements was fecundity (Møller, 1997). None of the species studied by Møller were nonhuman primates, so this type of work is prudent for understanding the relationship between FA and the environment. Others have examined the association of FA and environmental stress in small mammals and found that increased FA is associated with natural and anthropogenic environmental stressors (see review in Coda et al., 2017). Some of these studies measured FA by linear body measurements in live populations. Coda et al. (2017) found that with either geometric morphometric or linear measurements, FA is an accessible way to assess stress in mammals, hence its potential application to primate conservation.

5 CONCLUSION

In summary, the data presented here show that *Gorilla* and *Macaca* have more similar magnitudes of total cranial FA than *Pan*, which ultimately suggests that FA in the cranium may be more heavily influenced by environmental factors rather than taxonomic ones. Further, we see higher levels of variation in FA in *Macaca* and *Gorilla* than in *Pan* in this sample. Additionally, variation in FA across cranial regions and at each landmark across the cranium does not appear to be patterned by bone development or phylogenetic relationships. These results suggest that FA, or developmental instability more broadly, is more greatly influenced by environmental factors than genetic ones. Results also point to landmarks that are potentially more useful for future studies of FA in catarrhine primates.

Finally, these results have interesting potential applications to primate conservation and suggest that western lowland gorillas could have more urgent habitat conservation needs than central chimpanzees based on their ability to buffer stress.

ACKNOWLEDGMENTS

First, we thank the editors and reviewers for their constructive and helpful feedback on this manuscript. We also thank the Smithsonian's Division of Mammals (Dr. Kristofer Helgen) and Human Origins Program (Dr. Matt Tocheri) for the scans of USNM specimens used in this research (<http://humanorigins.si.edu/evidence/3d-collection/primate>). These scans were acquired through the generous support of the Smithsonian 2.0 Fund and the Smithsonian's Collections Care and Preservation Fund. Additionally, we thank the Cleveland Museum of Natural History's Physical Anthropology Department (Dr. Yohannes Haile-Selassie and Lyman Jellema) for access to the nonhuman primate specimens in the Hamann-Todd collection used to create 3D surface models for this study. Further, we would like to thank Dr. Lawrence Heaney and Adam Ferguson of the Field Museum of Natural History (FMNH) for access to the macaque specimens used in this research. Finally, we thank the following for their feedback and support: Dr. Lucas Delezene, Dr. Jerome Rose, and Caitlin Yoakum. The macaque sample was collected using funding from the National Science Foundation (NSF BCS 1551669 [Siobhán B. Cooke], NSF BCS 1551772 [Claire A. Kirchhoff], NSF BCS 1551766 [Claire E. Terhune]).

CONFLICT OF INTEREST

The authors declare no conflict of interest.

AUTHOR CONTRIBUTIONS

Ashly N. Romero: Conceptualization (equal); data curation (lead); investigation (lead); writing – original draft (lead); writing – review and editing (lead). **D. Rex Mitchell:** Formal analysis (supporting); methodology (supporting); writing – review and editing (equal). **Siobhán B. Cooke:** Writing – review and editing (equal). **Claire A. Kirchhoff:** Writing – review and editing (equal). **Claire E. Terhune:** Conceptualization (equal); investigation (supporting); supervision (lead); writing – review and editing (lead).

DATA AVAILABILITY STATEMENT

The specimen list with demographic information and Procrustes FA scores used in this project are supplied in **Data S1** (Tables **S1** and **S2**). The cranial 3D surface scans from the Natural Museum of Natural History used in this project are available upon request from Matt Tocheri. Surface scans taken by ANR are available in the Morphosource.org repository in the “Romero MA Thesis Scans” project and may be downloaded after obtaining written permission from the Cleveland Museum of Natural History. Scans of all macaque specimens included in this study are freely available on Morphosource.org in the “Normal and pathological covariation in the masticatory apparatus of anthropoid primates” project.

Supporting Information

Filename	Description
ajpa24432-sup-0001-supinfo.docx	Word 2007 document , 48.1 KB Data S1. Supporting information.

Please note: The publisher is not responsible for the content or functionality of any supporting information supplied by the authors. Any queries (other than missing content) should be directed to the corresponding author for the article.

REFERENCES

- Adams, D., Collyer, M., & Kaliontzopoulou, A. (2020). Geomorph: Software for geometric morphometric analyses. R package version 3.2.1. <https://cran.r-project.org/package=geomorph>
- Clarke, G. M. (1998). The genetic basis of developmental stability. V. Inter- and intra-individual character variation. *Heredity*, **80**(5), 562– 567.
- Coda, J. A., Martínez, J. J., Stienmann, A. R., Priotto, J., & Gomez, M. D. (2017). Fluctuating asymmetry as an indicator of environmental stress in small mammals. *Mastozoología Neotropical*, **24**(2), 313– 321.
- DeLeon, V. (2007). Fluctuating asymmetry and stress in a medieval Nubian population. *American Journal of Physical Anthropology*, **132**, 520– 534.
- Delgado-Acevedo, J., & Restrepo, C. (2008). The contribution of habitat loss to changes in body size, allometry, and bilateral asymmetry in two *Eleutherodactylus* frogs from Puerto Rico. *Conservation Biology*, **22**(3), 773– 782.
- Emlen, J., Freeman, D., & Graham, J. (1993). Nonlinear growth dynamics and the origin of fluctuating asymmetry. *Genetica*, **89**, 77– 96.
- Emlen, J., Freeman, D., & Graham, J. (2003). The adaptive basis of developmental instability: A hypothesis and its implications. In M. Polak (Ed.), *Developmental instability: Causes and consequences*. Oxford University Press.
- Folstad, I., Arneberg, P., & Karter, A. J. (1996). Antlers and parasites. *Oecologia*, **105**, 556– 558.
- Gómez-Robles, A., Hopkins, W. D., & Sherwood, C. C. (2013). Increased morphological asymmetry evolvability and plasticity in human brain evolution. *Proceedings of the Royal Society B*, **280**, 20130575.
- Graham, J., Raz, S., Hel-Or, H., & Nevo, E. (2010). Fluctuating asymmetry: Methods, theory, and applications. *Symmetry*, **2**(2), 466– 540.
- Guillerme, T., & Weisbecker, V. (2019). landvR: Tools for measuring landmark position variation. Zenodo. doi:<https://doi.org/10.5281/zenodo.2620785>.
- Hallgrímsson, B. (1993). Fluctuating asymmetry in *Macaca fascicularis*: A study of the etiology of developmental noise. *International Journal of Primatology*, **14**(3), 421– 443.
- Hallgrímsson, B. (1995). *Fluctuating asymmetry and maturational spans in mammals: Implications for the evolution of prolonged development in primates* [Unpublished doctoral dissertation]. University of Chicago, Chicago, IL.
- Hallgrímsson, B. (1998). Fluctuating asymmetry in the mammalian skeleton: Evolutionary and developmental implications. In M. K. Hecht, R. J. Macintyre, & M. T. Clegg (Eds.), *Evolutionary biology* (Vol. **30**). Springer.
- Hallgrímsson, B. (1999). Ontogenetic patterning of skeletal fluctuating asymmetry in rhesus macaques and humans: Evolutionary and developmental implications. *International Journal of Primatology*, **20**(1), 121– 151.

- Hoffman, A. A., & Woods, R. E. (2003). Associating environmental stress with developmental instability: Problems and patterns. In M. Polak (Ed.), *Developmental instability: Causes and consequences*. Oxford University Press.
- Hoover, K. C., & Matsumura, H. (2008). Temporal variation and interaction between nutritional and developmental instability in prehistoric Japanese populations. *American Journal of Physical Anthropology*, **137**, 469– 478.
- Hopton, M. E., Cameron, G. N., Cramer, M. J., Polak, M., & Uetz, G. W. (2009). Live animal radiography to measure developmental instability in populations of small mammals after a natural disaster. *Ecological Indicators*, **9**, 883– 891.
- Hutchison, D. W., & Cheverud, J. M. (1995). Fluctuating asymmetry in tamarin (*Saguinus*) cranial morphology: Intra- and interspecific comparisons between taxa with varying levels of genetic heterozygosity. *Journal of Heredity*, **86**, 280– 288.
- Javed, A., Chen, H., & Ghori, F. Y. (2010). Genetic and transcriptional control of bone formation. *Oral and Maxillofacial Surgery Clinics of North America*, **22**(3), 283– 293.
- Jin, S., Sim, K., & Kim, S. (2016). Development and growth of the normal cranial vault: An embryologic review. *Journal of Korean Neurosurgical Society*, **59**(3), 192– 196.
- Joganic, J. L., Willmore, K. E., Roseman, C. C., Richtsmeier, J. T., Rogers, J., & Cheverud, J. M. (2012). Comparative quantitative genetic analysis of cranial capacity and craniofacial morphology in two closely related primate species. In Q. Wang (Ed.), *Bones, genetics, and behavior of rhesus macaques*. Springer.
- Jung, H., & von Cramon-Taubadel, N. (2018). Comparison of cranial fluctuating asymmetry between normal and pathological specimens from a modern Thai skeletal group. *Homo*, **69**(4), 188– 197.
- Klingenberg, C. P. (2003a). Developmental instability as a research tool: Using patterns of fluctuating asymmetry to infer the developmental origins of morphological integration. In M. Polak (Ed.), *Developmental instability: Causes and consequences*. (427– 442). Oxford University Press.
- Klingenberg, C. P. (2003b). A developmental perspective on developmental instability: Theory, models, and mechanisms. In M. Polak (Ed.), *Developmental instability: Causes and consequences*. (14– 34). Oxford University Press.
- Klingenberg, C. P. (2008). Morphological integration and developmental modularity. *Annual Review of Ecology, Evolution, and Systematics*, **39**, 115– 132.
- Klingenberg, C. P. (2011). MorphoJ: An integrated software package for geometric morphometrics. *Molecular Ecology Resources*, **11**(2), 353– 357.
- Klingenberg, C. P. (2015). Analyzing Fluctuating Asymmetry with Geometric Morphometrics: Concepts, Methods, and Applications. *Symmetry*, **7**(2), 843– 934.
- Klingenberg, C. P., Barluenga, M., & Meyer, A. (2002). Shape analysis of symmetric structures: Quantifying variation among individuals and asymmetry. *Evolution*, **56**(10), 1909– 1920.
- Klingenberg, C. P., & McIntyre, G. S. (1998). Geometric morphometrics of developmental instability: Analyzing patterns of fluctuating asymmetry with Procrustes methods. *Evolution*, **52**(5), 1363– 1375.
- Klingenberg, C. P., & Monteiro, L. R. (2005). Distances and directions in multidimensional shape spaces: Implications for morphometric applications. *Systematic Biology*, **54**(4), 678– 688.
- Leigh, S. R. (1996). Evolution of human growth spurts. *American Journal of Physical Anthropology*, **101**, 455– 474.

- Leung, B., Forbes, M. R., & Houle, D. (2000). Fluctuating asymmetry as a bioindicator of stress: Comparing efficacy of analyses involving multiple traits. *The American Naturalist*, **155**(1), 101– 115.
- Livshits, G., & Smouse, P. E. (1993). Multivariate fluctuating asymmetry in Israeli adults. *Human Biology*, **65**(4), 547– 578.
- Livshits, G., Yakovenko, K., Kletselman, L., Karasik, D., & Kobylansky, E. (1998). Fluctuating asymmetry and morphometric variation of hand bones. *American Journal of Physical Anthropology*, **107**, 125– 136.
- Mackie, E. J., Ahmed, Y. A., Tatarczuch, L., Chen, K. S., & Mirams, M. (2008). Endochondral ossification: How cartilage is converted into bone in the developing skeleton. *International Journal of Biochemistry and Cell Biology*, **40**, 46– 62.
- Marshall, A. J., & Wrangham, R. W. (2007). Evolutionary consequences of fallback foods. *International Journal of Primatology*, **28**, 1219– 1235.
- McGrath, J. W., Cheverud, J. M., & Buikstra, J. E. (1984). Genetic correlations between sides and heritability of asymmetry for nonmetric traits in rhesus macaques on Cayo Santiago. *American Journal of Physical Anthropology*, **64**, 401– 411.
- Møller, A. P. (1997). Developmental stability and fitness: A review. *The American Naturalist*, **149**(5), 916– 932.
- Morgan, D., & Sanz, C. (2007). Best practice guidelines for reducing the impact of commercial logging on great apes in western equatorial Africa (Report No. 34). Gland, Switzerland: IUCN Species Survival Commission.
- Mumby, H., & Vinicius, L. (2008). Primate growth in the slow lane: A study of inter-species variation in the growth constant *a*. *Evolutionary Biology*, **35**(4), 287– 295.
- Palmer, A. R. (1994). Fluctuating symmetry analyses: A primer. In T. A. Markow (Ed.), *Developmental instability: Its origin and evolutionary implications*. Springer.
- Palmer, A. R., & Strobeck, C. (1986). Fluctuating asymmetry: Measurement, analysis, patterns. *Annual Review of Ecology and Systematics*, **17**, 391– 421.
- R Core Team. (2017). *R: A language and environment for statistical computing*. R Foundation for Statistical Computing. <https://www.R-project.org/>
- Reddy, B. M. (1999). Fluctuating asymmetry and canalization: An appraisal based on a-b ridge counts among Indian populations with diverse backgrounds. *American Journal of Human Biology*, **11**, 367– 381.
- Robinson, C., & Terhune, C. E. (2017). Error in geometric morphometric data collection: Combining data from multiple sources. *American Journal of Physical Anthropology*, **164**, 62– 75.
- Scheuer, L., & Black, S. (2000). *Developmental juvenile osteology*. Academic Press.
- Schlager, S., & Rüdell, A. (2015). Analysis of the human osseous nasal shape – Population differences and sexual dimorphism. *American Journal of Physical Anthropology*, **157**, 571– 581.
- Singh, N., Harvati, K., Hublin, J., & Klingenberg, C. P. (2012). Morphological evolution through integration: A quantitative study of cranial integration in *homo*, *pan*, *gorilla*, and *Pongo*. *Journal of Human Evolution*, **62**, 155– 164.
- Van Dongen, S. (2015). Lack of correlation between fluctuating asymmetry and morphological masculinity/femininity in primate skulls. *International Journal of Primatology*, **36**, 113– 123.
- Van Valen, L. (1962). A study of fluctuating asymmetry. *Evolution*, **16**(2), 125– 142.
- von Cramon-Taubadel, N. (2009). Revisiting the homoiology hypothesis: The impact of phenotypic plasticity on the reconstruction of human population history from craniometric data. *Journal of Human Evolution*, **57**(2), 179– 190.

- von Cramon-Taubadel, N. (2011). The relative efficacy of functional and developmental cranial modules for reconstructing global human population history. *American Journal of Physical Anthropology*, **146**, 83– 93.
- von Cramon-Taubadel, N., & Smith, H. (2012). The relative congruence of cranial and genetic estimates of hominoid taxon relationships: Implications for the reconstruction of hominin phylogeny. *Journal of Human Evolution*, **62**(5), 640– 653.
- Wiley, D. F., Amenta, N., Alcantara, D. A., Ghosh, D., Kil, Y. J., Delson, E., Harcourt-Smith, W., Rohlf, F. J., St John, K., & Hamann, B. (2005). Evolutionary morphing. *Visualization IEEE*, 431– 438.
- Willmore, K. E., Klingenberg, C. P., & Hallgrímsson, B. (2005). The relationship between fluctuating asymmetry and environmental variance in rhesus macaque skulls. *Evolution*, **59**(4), 898– 909.
- Willmore, K. E., Young, N. M., & Richtsmeier, J. T. (2007). Phenotypic variability: Its components, measurement and underlying developmental processes. *Evolutionary Biology*, **34**, 99– 120.